DEUTSCHES ELEKTRONEN-SYNCHROTRON DESY

DESY SR 84-15
April 1984

EXAFS STUDY OF PRECIPITATES IN AlCu

by

B. Lengeler

Inst. f. Festkörperforschung, Kernforschungsanlage Jülich

P.M. Eisenberger

Corporate Research-Science Lab., Exxon Res. & Eng. Co., Linden, New York

ISSN 0723-7979

NOTKESTRASSE 85 · 2 HAMBURG 52

DESY SR 84-15
April 1984

ISSN 0723-7979

EXAFS STUDY OF PRECIPITATES IN AlCu

B. Lengeler[+] and P.M. Eisenberger[*]

[+] Institut für Festkörperforschung, Kernforschungsanlage Jülich, Postfach 1913, D-5170 Jülich, West Germany

[*] Corporate Research-Science Laboratories, Exxon Research and Engineering Company, Linden, N.J. 07036, USA

Introduction

When an AlCu alloy with up to 2.5 at% Cu is quenched from about 540 °C to room temperature it decomposes through a series of metastable precipitates. These are the Guinier-Preston I (GPI) zones, the Guinier-Preston II (GPII or Θ") zones and the phase Θ'. The equilibrium precipitate is the phase Θ of composition $CuAl_2$. The GPI and GPII zones are coherent with the matrix and are responsible for the hardening of the alloy (1). In this paper we are concerned with the supersaturated solid solution (SSSS) and the GPI zones. The GPI zones are platelets on {100} lattice planes up to 5 nm in diameter which distort the surrounding lattice. They dissolve within seconds at 200 °C (reversion). Depending on the time for which the alloy is kept at 200 °C the Cu goes in solution or more stable precipitates are formed. Despite the numerous publications done so far on GPI zones (reviewed e.g. in references 1,2) there are a number of open questions: 1. What is the fraction X of Cu in the alloy precipitating into zones? 2. What is the fraction α of Cu in each platelet? 3. What is the number n of layers in a GPI zone? How do X, α and n depend on the initial concentration c_o of Cu and on the annealing temperature T_A? 4. What is the amount of displacement of the neighboring Al planes? In a recent small angle neutron scattering (SANS) investigation of GPI zones it was found (2) that the product $X\alpha n$ depends strongly on the Cu concentration c_o and on the ageing temperature T_A. $X\alpha n$ is always substantially smaller than 1. For alloys annealed at 22 °C $X\alpha n$ is 0.66 at 2.3 at% Cu and 0.42 at 1 at% Cu. In SANS only the product $X\alpha n$ could be determined, but not the individual factors. The combination of the SANS and of the present EXAFS investigation will enable us to determine the individual factors X, α and n and the lattice distortion of the first neighboring Al plane.

EXAFS spectroscopy

The X-ray absorption coefficient $\mu(E)$ in condensed matter shows a fine structure (EXAFS) above the different absorption edges. This effect can be used as a local probe giving interatomic distances r_j and coordination numbers N_j for the j-th shell around the atom which absorbs the photon of energy E(3-5). If we denote by k the wave vector of the photoelectron which was bound with energy E_o

$$k = \frac{2m}{\hbar^2} \sqrt{(E-E_o)} \qquad (1)$$

the modulation $\chi(k)$ in the absorption coefficient reads

$$\chi = \sum_j \frac{1}{kr_j^2} N_j F_j(k) D_j \exp(-2\sigma_j^2 k^2) \sin(2kr_j + \phi_j(k)) \qquad (2)$$

---

submitted to Scripta Met.

ISSN 0723-7979

In the present case we have measured the EXAFS at the K edge of Cu in different AlCu alloys. $F_j(k)$ is the amplitude with which the photoelectron is scattered back from the Al and Cu neighbors surrounding the absorbing Cu atom and $\phi_j(k)$ is the corresponding change in phase occuring in the absorber and backscatterers. D_j is a factor taking care of inelastic losses and σ_j^2 a Debye-Waller factor. We have determined $F_j(k) \cdot D_j$ and $\phi_j(k)$ from model compounds (metallic copper for Cu-Cu pairs and $CuAl_2$, NiAl and CoAl for Cu-Al pairs).

Experimental details

The samples used in the present investigation were polycrystalline foils of 100 µm thickness with 0.5, 1, 2 and 2.3 at% Cu. They were homogenized at 540 °C in a He atmosphere and quenched to -60 °C (for preparing SSSS) or to room temperature (for precipitating GPI zones). Since a SSSS of AlCu starts to decompose at about -30 °C due to vacancy migration, a high cooling rate (30000 °C/sec) and a low bath temperature (-60 °C) are necessary to quench-in the equilibrium state present at 540 °C (6). The samples containing GPI zones were aged for 30 days at room temperature. A sample with 2.3 at% Cu was annealed for 20 hours at room temperature and for 6 hours at 243 °C in order to precipitate the phase Θ'. The model compounds $CuAl_2$, CoAl and NiAl were prepared by melting appropriate amounts of the elements in a cold crucible in purified argon.

The EXAFS were measured in transmission at the Hamburger Snychrotronstrahlungslabor (beam line ROEMO) and at the Stanford Synchrotron Radiation Laboratory. Si(111) double crystal monochromators with an energy resolution of about 2 eV at the K edge of Cu were used. All measurements were done at 77 K.

Experimental results

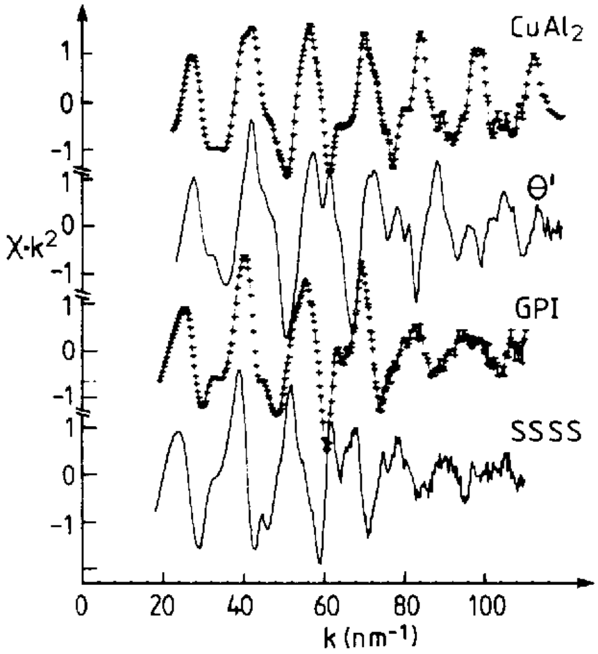

FIG 1:
EXAFS $\chi \cdot k^2$ for $CuAl_2$ and for AlCu (2.3 at% Cu) with phase Θ', with GPI zones and as supersaturated solid solution (SSSS).

Figure 1 shows the EXAFS $\chi \cdot k^2$ versus k for the SSSS, for GPI zones, for the phase θ' and for $CuAl_2$. The changes in the alloys during the decomposition are clearly visible in the EXAFS. The values for E_o used in Eq. (1) were chosen to be at the first inflection point in the K edges. The scattering amplitudes and phases for Cu-Cu pairs used in Eq. (2) were extracted from metallic Cu. The model compounds used to extract the amplitudes and phases for Cu-Al pairs were CoAl and NiAl which have CsCl structure. The amplitudes and phases which vary only slowly with the atomic number Z (7) were extrapolated from Co-Al and Ni-Al to Cu-Al. A consistency test with these data on the structure of $CuAl_2$ (which has Cu and Al neighbors in the first coordination shell around a Cu atom) gave satisfactory results.

We now proceed with the results obtained on the SSSS. A detailed analysis of the first neighbor distances r_1 around a Cu atom is shown in figure 2. Note that r_1 shows a linear dependence on the Cu concentration c_o. In dilute AlCu ($c_o \rightarrow 0$) the first shell of Al neighbors is at (0.280 ± 0.001)nm compared to a first neighbor distance of 0.285 nm in pure Al. The smaller atomic volume of Cu compared to that of Al produces a contraction s_1 of the first Al shell by $-(0.005 \pm 0.001)$nm. Besides the local lattice distortion s_1 (measured in EXAFS) the Cu impurities in Al create a lattice contraction $\Delta V/V_z c_o$ which can be determined by lattice parameter measurement. Dorn et al (8) found in dilute AlCu alloys (with c_o below 0.1 at% Cu).

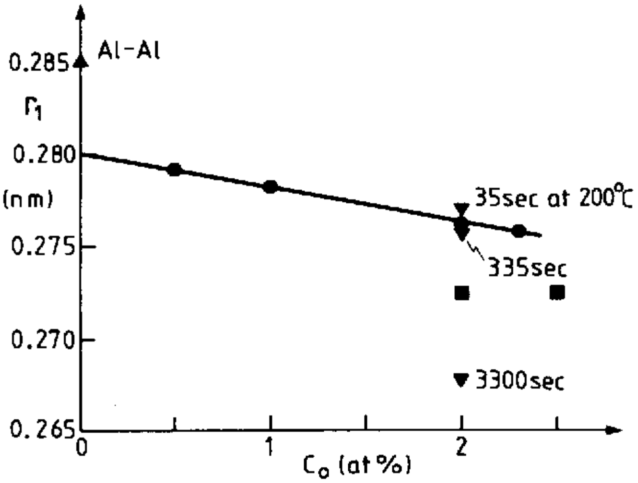

FIG 2:
First neighbor distance r_1 in SSSS of AlCu (circles). The results by Fontaine et al (11) are shown as squares. The triangles (▼) show the result for reverted alloys kept for 35, 335 and 3300 seconds at 200 °C.

$$\frac{\Delta V}{V_z c_o} = -0.41 \pm 0.06 \qquad (3)$$

In an cubic elastic medium (like Al) the local contraction s_1 and the lattice parameter contraction $\Delta V/V_z c_o$ are related by (9-10)

$$s_1 = -\frac{\sqrt{2}}{12} (c_{11}+2c_{12}) a^3 \sum_i G_{1i|i} \frac{\Delta V}{V_z c_o} \qquad (4)$$

The elastic constants $(c_{11}+2c_{12})$ for Al have the value $2.284 \cdot 10^{12}$ dyn/cm^2. a is the lattice constant of Al. The static Greens functions G_{ij} and $G_{ij|j}$ have been calculated by Schober (10). Using his data Eq. (4) reads

$$s_1 [\mathrm{nm}] = 0.0123 \ \frac{\Delta V}{V_z c_o} \qquad (5)$$

Inserting Eq. (3) in Eq. (5) we obtain for the local lattice distortion s_1 obtained from lattice parameter measurements the value $s_1 = -(0.005\pm0.001)$nm, in very good agreement with the result obtained by EXAFS. In an earlier EXAFS study on AlCu alloys Fontaine et al (11) found an interatomic distance r_1 in a solid solution of 0.2725 nm, (figure 2). The corresponding distortion s_1 in the first shell is 2.5 times larger than that observed in the present investigation. What Fontaine et al claim to be a solid solution was in reality a sample with GPI zones which were reverted for 2 months at 190 °C. We have also analyzed the interatomic distances of alloys with GPI zones which were reverted for different amounts of time (35, 335 and 3300 sec) at 200 °C. The result is shown in figure 2. Shortly after reversion the interatomic distance r_1 is very similar to that in a SSSS. But already after 1 hour at 200 °C the state of the alloy is no longer that of a SSSS. We feel that the samples used in the present investigation which were quenched to a temperature where the vacancy migration is suppressed were really SSSS of AlCu.

We attribute the decrease in the first neighbor distance r_1 with c_o in figure 2 to short range order (SRO) in the SSSS. An analysis of the alloy with 2.3 at% Cu gives 1 to 2 additional Cu atoms next to a given Cu atom. Matsubara and Cohen (12) found by diffuse X-ray scattering in an alloy with 1.7 at% Cu at 520 °C that the Cu atoms tend to form small Cu-rich clusters of various shapes. Our result agrees qualitatively with this observation.

We now proceed with the analysis of the structure of the GPI zones. When a supersaturated AlCu alloy decomposes at room temperature, not all the Cu atoms precipitate into GPI zones but some will stay in solution. The fraction X which precipitates into GPI zones depends on the initial Cu concentration c_o and on the ageing temperature T_A. This fraction has to be known in order to analyse the EXAFS data correctly. We have extracted this number from the SANS analysis mentioned above (2) which gave $X\alpha n = 0.66$ for $c_o = 2.3$ at% and 0.42 for 1 at% Cu. Figure 3a shows the EXAFS for AlCu with 1 and 2.3 at% Cu annealed for one month at room temperature. We do not expect the two curves to be identical since the product $X\alpha n$ and as we will see the fractions X are not equal in both alloys. We have decomposed the measured EXAFS χ_{meas} (figure 3a) according to

$$\chi_{meas} = X \ \chi_{GPI} + (1-X) \ \chi_{SSSS} \qquad (6)$$

where χ_{SSSS} is the EXAFS for the SSSS and χ_{GPI} the contribution for the GPI zones alone. The best agreement for the GPI contribution of alloys with 1 and 2.3 at% is obtained for X = 0.66 at 2.3 at% and X = 0.42 at 1 at% Cu. This corresponds to $n=\alpha=1$ (monolayered GPI zones of pure copper). The result of this decomposition is shown in figure 3b. We have analysed these EXAFS with a two shell fit (Al and Cu neighbors with 4 free parameters: two distances and two coordination numbers). The results are summarized in table 1. The following points are noteworthy.

(1) The distance from a Cu atom in a GPI zone to its first Al neighbors is (0.263 ± 0.002)nm. This corresponds to a 16 % shrinkage of the neighboring Al planes towards the Cu platelet. This agrees well with the value of 17 % quoted by Fontaine et al (11) for this parameter. On the other hand, Gerold (13) found a shrinkage of only 10 %.

(2) The fit shows the Cu atoms in the platelet to occupy Al sites with an interatomic distance of 0.285 nm.

(3) In the average a Cu atom has 3.5 other Cu atoms as first neighbors. This is what we expect for monolayered GPI zones of pure Cu on Al {100} planes. The expected number is smaller than 4 due to the finite size of the GPI zones (diameters of 2.16 and 2.64 nm for 1 and 2.3 at% Cu (2)) in which an appreciable fraction of Cu atoms are located at the edge of the zones.

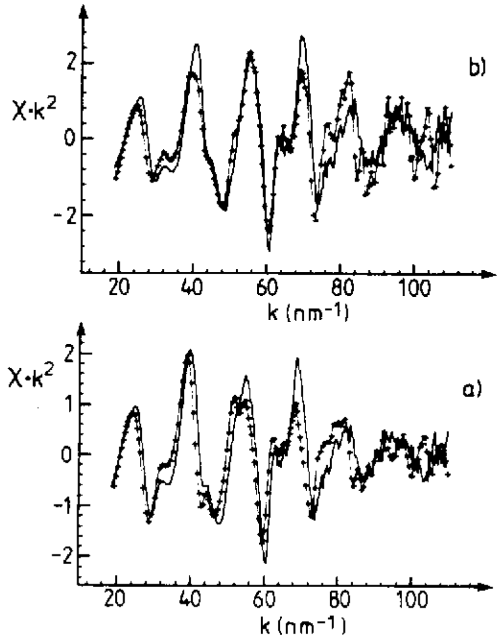

FIG 3:
EXAFS $\chi \cdot k^2$ for AlCu with 2.3 at% (full line) and 1 at% (crosses) copper containing GPI zones:
a) as measured and
b) after the decomposition according to Eq. (6).

TABLE 1: First Shell Distances r_1 and Coordination Numbers N_1 around Cu in GPI Zones in AlCu.

c_o (at%)	r_1(nm)	N_1	r_1(nm)	N_1
2.3	0.263 ± 0.002	10 ± 2	0.285 ± 0.002	3.8 ± 1
1	0.265 ± 0.002	8 ± 2	0.286 ± 0.002	3.5 ± 1

This result supports the decomposition according to Eq. (6) found in figure 2.

The result found in the present investigation is in contradiction to the conconclusion made by Fontaine et al (11). These authors found that the GPI zones in AlCu are monolayers with an average composition of 50 % Cu and 50 % Al. Since Fontaine et al used an incorrect model for the solid solution in their analysis of the GPI zones (see figure 2) it is not supprising that their result differs from the present one. Our result is also in contradiction to a diffuse X-ray scattering investigation by Auvray et al (14). These authors found the GPI zones to be a mixture of single and multilayer zones of pure Cu. This would imply a Cu-Cu coordination larger than 4. We have found no evidence for this in our analysis for a decomposition as in Eq. (6). Assuming $X = 1$ gives also N_1 smaller than 4. At the present time we have no explanation for this discrepancy, unless we assume that the long ageing time of 12 years used in reference 14 has created a different state of decomposition in their alloy compared to the alloys used in this investigation.

Conclusions

The results of the present EXAFS investigation on AlCu can be summarized as follows:

(1) In order to prevent the decomposition of a supersaturated solid solution (SSSS) of AlCu it is necessary to quench the alloy to temperatures below −30 °C. SSSS show short range order. In the dilute limit the lattice distortion s_1 of the first Al coordination shell around a Cu atom is −(0.005± 0.001)nm. This result agrees well with the value deduced from lattice parameter measurements.

(2) The fraction X of Cu precipitating into GPI zones in AlCu depends on the initial Cu concentration c_o and on the ageing temperature. The remaining Cu stays in solution. At room temperature 66 % of the Cu in an alloy with 2.3 at% Cu precipitates into GPI zones. At 1 at% Cu the fraction is only 42 %.

(3) GPI zones in AlCu are monolayers of pure Cu with Cu occupying Al sites. The shrinkage of the neighboring Al planes towards the Cu platelets is 16 %. Of all the models proposed so far for GPI zones the present model agrees best with that proposed by Gerold (13).

(4) AlCu alloys with GPI zones which are reverted at 200 °C resemble a SSSS only within the first 100 seconds. After an hour at 200 °C a state different from a SSSS is reached.

Acknowledgements

The authors are indebted to the members of Hasylab and SSRL for the help during the measurements.

References

1. A. Kelly and R.B. Nicholson, Prog. Mat. Sci. 10, 289 (1963).
2. P. Prieto, B. Lengeler and D. Schwahn, Acta met. (1984).
3. P.A. Lee, P.H. Citrin, P. Eisenberger and B.M. Kincard, Rev. Mod. Phys. 53, 969 (1981).
4. B.K. Teo and D.C. Joy (ed.) EXAFS Spectroscopy, Techniques and Applications, Plenum Press (1981).
5. A. Bianconi, L. Incoccia and S. Stipcich (ed.) EXAFS and Near Edge Structure, Springer Series in Chemical Physics, Vol. 27 (1983).
6. B. Lengeler, Phil. Mag. 34, 259 (1976).
7. B.K. Teo and P.A. Lee, J. Amer. Chem. Soc. 101, 2815 (1979).
8. J.E. Dorn, P. Pietrokowsky and T.E. Tietz, J. Metals 2, 933 (1950).
9. G. Leibfried and N. Breuer, Point Defects in Metals I, Springer Tracts in Modern Physics 81 (1978).
10. J.W. Deutz and H.R. Schober, Comput. Phys. Comm. 30, 87 (1983) and private communication.
11. A. Fontaine, P. Lagarde, A. Naudon, D. Raoux and D. Spanjaard, Phil. Mag. 40, 17 (1979).
12. E. Matsubara and J.B. Cohen, Acta metall. 12, 2129 (1983).
13. V. Gerold, Z. Metallkde 45, 593, 599 (1954).
14. X. Auvray, P. Georgopoulos and J.B. Cohen, Acta Metall. 29, 1061 (1981).